Indonesian Journal of Aerospace Vol. 21 No. 2 December 2023 : pp 99–108 (Pinindria et al.)
DOI: 10.55981/ijoa.2023.900
https://ejournal.brin.go.id/ijoa/

Impact of Airfoil Section on Winglet Design for Enhancing Aerodynamics Performance of Aircraft using CFD Analysis

Sinung Tirtha P.[1], Arifin Rasyadi S.[1], Muhammad Fajar[1], Kurnia Hidayat[1], Jefri Abner H.[1], Mohamad Luthfi R.[2]

[1]Research Center for Aeronautics Technology – BRIN, Indonesia
[2]Research Center for Intelligent Mechatronics – BRIN, Indonesia
e-mail: sinung.tirtha.pinindriya@brin.go.id

Received: 06-07-2023 Accepted: 28-11-2023 Published: 31-12-2023

Abstract

This research paper investigates the influence of airfoil section on winglet design to enhance aerodynamic performance while considering structural aspects. The selection of the airfoil section significantly affects the distribution of lift and drag along the winglet, influencing the overall lift-to-drag ratio of the aircraft and its ability to reduce drag by smoothing the airflow over the wingtip. Three airfoil sections, namely NACA 0010 (symmetrical), NACA 64-009 (thin cambered), and PSU 94-047 (cambered), were compared using computational fluid dynamics (CFD) simulations. The study examines the forces and moments experienced by the winglet, including drag force, lift force, on the wing surface. The CFD simulations were conducted using a Computational Wind Tunnel (CWT) tool, which employs numerical methods and mathematical models to analyze fluid flow around objects. The solver code is based on RANS method. The wind tunnel testing is provided to validate one of the CFD simulation results. The findings indicate that the installation of winglets increases both the lift-to-drag ratio compared to the clean wing configuration. Among the studied airfoil profiles, NACA 0010 demonstrated the optimum lift-to-drag ratio, showing a 9.5% improvement over the clean wing configuration. Although it is a symmetrical airfoil, the thickness of NACA 0010 contributes to higher lift production compared to the cambered airfoils (NACA 64-009 and PSU 94-047), which show approximately a 10% improvement in lift-to-drag ratio. While the differences in aerodynamic characteristics between the airfoil profiles are marginal, the overall addition of winglets proves effective in increasing lift and reducing induced drag. The research highlights the significance of airfoil shape and thickness in optimizing winglet performance. Future studies should focus on refining the winglet airfoil profile to maximize the benefits derived from both thickness and cambered shape, aiming to further enhance aerodynamic efficiency.

Keywords: winglet design, airfoil, CFD simulation, experimental aerodynamics.

1. Introduction

An aircraft comprises several major components, one of which is a wing. The main function of the wing is to generate the aerodynamic force of lift to keep the aircraft airborne (Sadrey, 2012), but the lower pressure air above the wing and the higher-pressure air below seek to balance out, causing the spiraling airflow called wingtip vortices (Tirtha et.al., 2020). These vortices are responsible for the appearance of Induced Drag (Rabbi et.al., 2015). It is imperative to reduce induced drag because if an airplane experiences less drag, it will require less power and therefore less fuel to fly an arbitrary distance, thus making flight commercial and otherwise more efficient and less costly (Altab et.al, 2012). To reduce induced drag, a device called a winglet is placed vertically at a set angle on the wingtip of the aircraft (Sidairi et.al, 2016)(Sawale et.al, 2017).

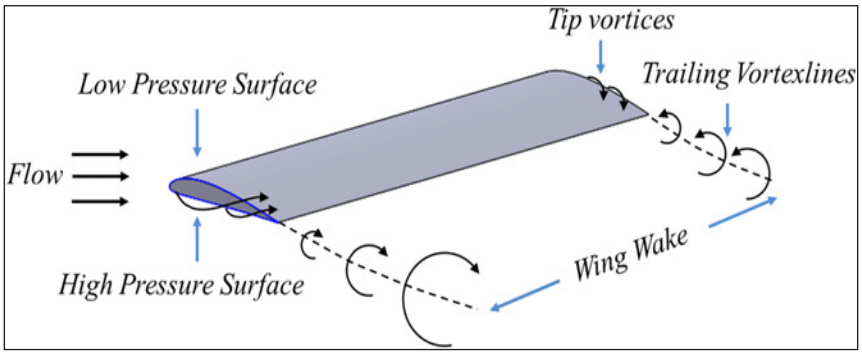

Figure 1-1. Wingtip Vortices over a wing section (Guha et.al, 2015)

In 1976, Whitcomb proposed new wingtips which he called winglets to observe the aerodynamic effect in practice. He found that the winglets reduced the induced drag by about 20% with an increase in wing lift-drag ratio by 9% for Mach number 0.78 and near the design lift coefficient (Whitcomb, 1976). In 1979 and 1980 Whitcomb installed and flight-tested a small vertical winglet on Boeing KC-135A aircraft, and the results are based on the theory that almost all wings are vertical at the tip of the wing can give a lower trailing vortex strength if the design is accurate. Winglets, however, introduce giant masses into the principal wing structure, which could decrease the anticipated advantages. These additional loads result in a heavier design, new wingtip interfaces, and an overall re-engineering of the wing box to allow for the winglet surface integration (Verrastro and Dimino, 2018). The induced drag created at the wingtips can be reduced by placing a winglet at the wingtips, leads to an increase in L/D ratio and increases fuel efficiency (Ravi and Kishore, 2016).

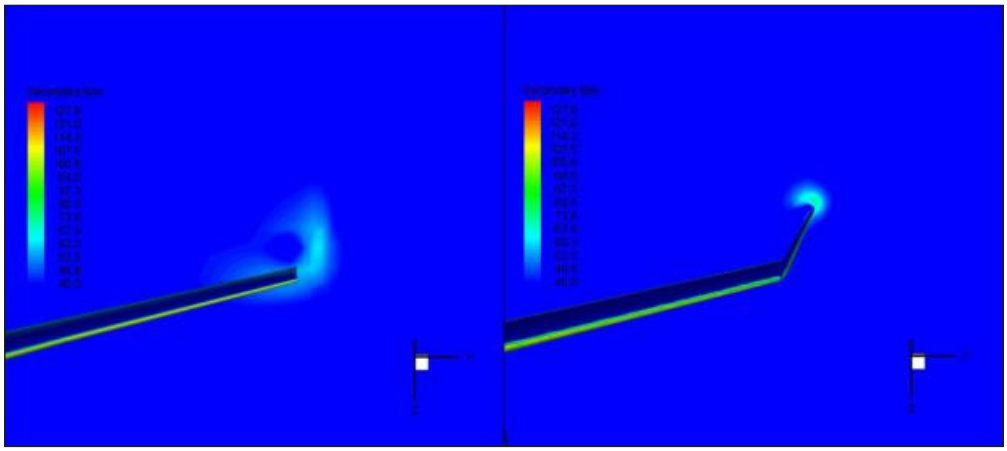

Figure 1-2. Simulation example of Wingtip vortices with or without winglet (Kim, 2010)

Figures 1-2 show that the effect of adding winglets is that the vortex generated at the wingtip becomes smaller than that without winglets, the induced drag is reduced due to the smaller tip vortex, and there is an increase in the lift coefficient by 6.8% and 11.9% at angles of attack of 0° and 10°. However, it should be noted that the addition of a winglet to reduce drag and increase wing efficiency also produces unavoidable bending moments in the wing structure, so it needs attention in structural design, as studies that have been conducted by several previous researchers (Krog et.al, 2004)(Bontoft, 2018)(Singh et.al, 2016)(Teixeira et.al, 2016)(Maughmer et.al, 2002).

The airfoil section may play a critical role in winglet design by affecting the amount of lift and drag that a winglet produces. The selection of the airfoil section influences the distribution

of lift along the span of the winglet, which affects the overall lift-to-drag ratio of the aircraft. The choice of airfoil section also affects the winglet's ability to reduce drag by smoothing the airflow over the wingtip. This research paper investigates the impact of airfoil section on winglet design for aerodynamic performance improvement while also makes a consideration to wing structural design. This paper discusses the importance of airfoil section in winglet design, the benefits of choosing the right airfoil section, and the challenges in optimizing winglet design with the appropriate airfoil section.

2. Methodology

2.1. Winglet Design

This research compared three different types of airfoil sections for the designed winglet. These airfoils are a symmetrical airfoil of NACA 0010, a thin cambered airfoil of NACA 64-009, and a cambered airfoil of PSU 94-047 (Maughmer et.al, 2002). The selection of this type of airfoil is based on several references that have used winglets on the aircraft (Maughmer et.al, 2002) (Mathew et.al, 2020) (Lehmkuehler, 2015). An asymmetrical or cambered airfoil has an upper curve more curved than the bottom curve of the airfoil surface, so it creates more lift. This type of airfoil at an angle of attack 0 already has a lift coefficient (Anderson, 2017). A cambered airfoil is the most common shape of conventional aircraft. The three airfoils used for winglet design (Figure 2-1) will be studied using CFD simulation method, with one case validated using experimental method in a wind tunnel. In previous research, a study was also conducted on the wing of this 19-passenger commuter aircraft with and without winglets with can angle variations using the CFD approach (Aribowo et.al, 2012).

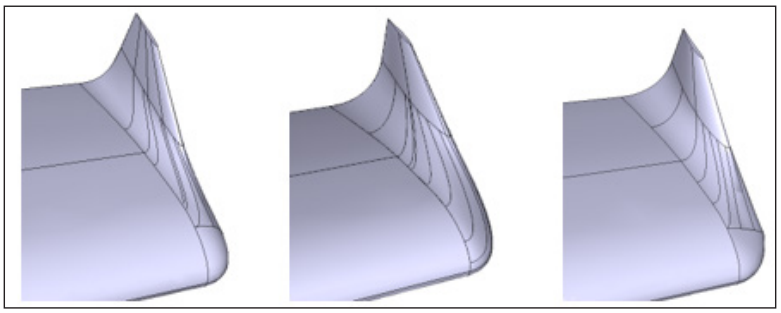

Figure 2-1. Winglet using (a) NACA 0010, (b) PSU 94097, (c) NACA 64009

2.2. Simulation Validation Method

This research investigates the use of wind tunnel testing for aerodynamic validation. The wind tunnel used is an open circuit type. The maximum speed that can be used is about 60 m/s, with a cross-sectional area of 2,75 x 1,75 m and the total length of the test section is 10 m. In wind tunnel testing, the things that need to be known are the forces and moments experienced by the test object. These forces and moments are drag force, lift force, side force, pitch moment, yaw moment, and roll moment (Hamonangan and Fajrin, 2015). That is shown in Figure 2-2.

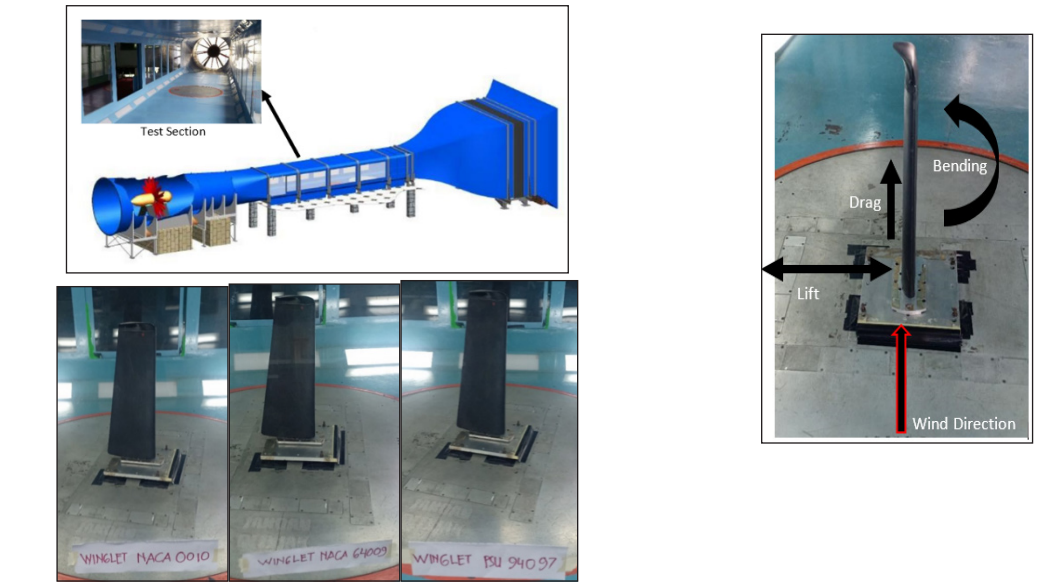

(a) Wind Tunnel Facility and Wing Mockup for Validation

(b) Force and Moment Measurement Method

Figure 2-2. Forces and Moments

The test on this wind tunnel is a wing model that is installed in half because of its symmetry so that it can represent the whole. The wings are mounted standing so that the force acting on the turntable is or will be used, namely the side force that will be processed as lift, drag, and yaw moments as pitch moments. As can be seen in the picture below.

The winglet test model for wind tunnel testing is made to a scale of 1:6.3 from its original size. The material used to make the test model is in accordance with the testing standard, namely with a solid aluminum material so that the test results data are valid.

2.3. Computational Wind Tunnel

Computational Wind Tunnel (CWT) is a powerful virtual simulation tool that is used to model and analyze the aerodynamic performance of an object. CWT is based on Computational Fluid Dynamics (CFD), a field of study that uses numerical methods and mathematical models to simulate fluid flow. CWT simulations can be used to study a wide range of fluid dynamics problems, like the flow of air around an aircraft wing and on a winglet. One of the most used CFD methods is the Reynolds-Averaged Navier-Stokes (RANS) method, which is used to solve the Navier-Stokes equations that describe the motion of fluids. The RANS method is a time-averaged approach to solving the Navier-Stokes equations. It assumes that the fluid flow is steady and that the flow variables can be decomposed into time-averaged and fluctuating components. The time-averaged equations are then solved numerically to obtain the mean flow field, while the fluctuating components are modeled using turbulence models. The governing equations of fluid flow are the Navier-Stokes equations, which describe the conservation of mass, momentum, and energy in a fluid. The RANS method uses turbulence models to simulate the behavior of turbulent flow, which can be important for designing and optimizing engineering systems that operate under turbulent conditions. The governing equations of Navier-Stokes are simplified for this study and consist of mass conservation (2-1) and momentum equations as a vector (2-2).

$$\frac{\delta \rho}{\delta t} + \nabla \cdot (\rho v) = 0 \tag{2-1}$$

$$\rho \left(\frac{\delta v}{\delta t} + v \cdot \nabla v \right) = -\nabla p + \nabla \cdot \left(\mu \cdot (\nabla v + (\nabla v)^T) \right) + \nabla (\lambda \nabla \cdot v) \tag{2-2}$$

This study used the computational domain of the wind tunnel and scaled wing-winglet component. The CFD solver used is a non-commercial RANS solver. For the turbulence model, the k-omega SST method is used.

3. Result and Analysis

3.1. Simulation Setting

Simulation of CWT is performed on a certain fluid domain as a representation of the physical wind tunnel. A structural grid or mesh has been generated on the fluid domain. To determine whether the simulation results are independent of the grid size, a grid convergence test has been conducted, as shown in Figure 3-1 (a). The graph shows that from a grid size of two million to three million elements, there is no significant change in the aerodynamic coefficients, especially the drag coefficient. So, the selected grid size is approximately three million elements. The fluid domain is enclosed by a boundary condition shown in Figure 3-1 (b). The atmospheric condition on that fluid domain also represents the condition at experimental testing. The detailed atmospheric condition is shown in Table 3-1 (a), and the boundary type is shown in Table 3-1 (b).

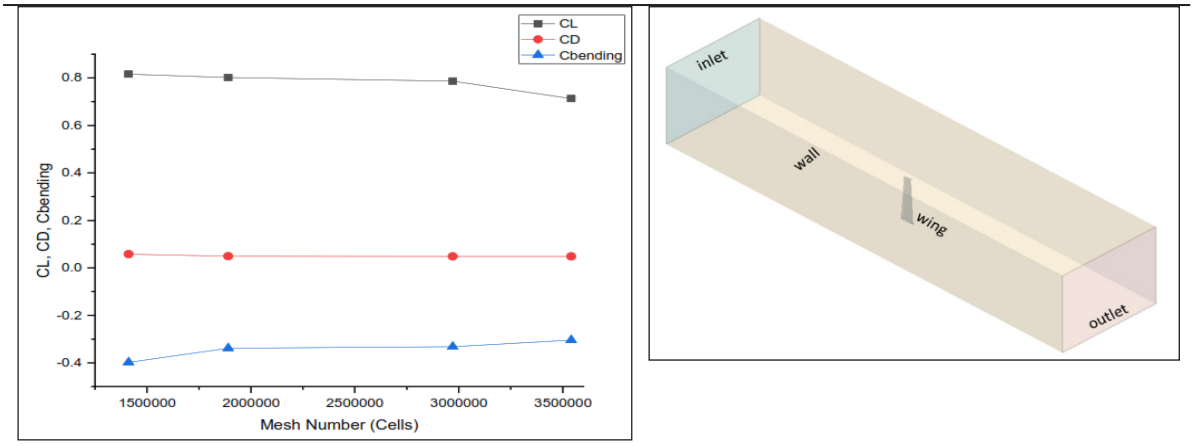

(a) Grid Convergence Test Results **(b) Fluid Domain and Boundary Condition**

Figure 3-1. Grid convergence and domain condition

Table 3-1. Atmospheric and boundary condition on simulation

(a) Atmospheric Condition Values on Simulation

PHYSICAL CONDITIONS

Parameter	Value	Units	Remark
Fluid Type	Air		at ISA +15 C
Density	1,154	kg/m3	
Viscosity	1.85E-05	Pa.s	dynamic viscosity
Ambient Pressure	96500	Pa	
Constant Velocity	30	m/s	Tunnel Velocity
Wing Reference Area	0.124	m2	
Angle of Attack	-4 to 24	deg	Sweep / Variaton

(b) Boundaries Condition Type and Values on Simulation

BOUNDARIES

Name	Type	Value	Units
Tunnel Inlet	Velocity Inlet	30	m/s
Tunnel Outlet	Pressure Outlet	96.500	Pascal
Tunnel Wall	No Slip Wall	0	m/s
Tunnel Model (Wing)	No Slip Wall	0	m/s

3.2. Simulation Results and Validation

The sweep angle of attack is performed on the CWT simulation to obtain force and moment from the four configurations of winglet study, consisting of a clean wing, a wing with winglet NACA 0010, winglet PSU 94097, and winglet NACA 64009. The wing lift force and drag force are calculated as aerodynamic coefficients for comparison, shown in a series of figures below.

Figure 3-2 (a) shows a comparison of lift coefficient with the angle of attack variation with and without winglet. The winglet design with NACA 0010 airfoil profile has a higher maximum lift and lower angle of stalls than the others. Wind tunnel test results of a test model of a winglet with NACA 0010 are shown in this figure (blue point) to provide validation and verification purposes. The result shows a similar trend in the linear region, but only at zero angle of attack the magnitudes are close to each other.

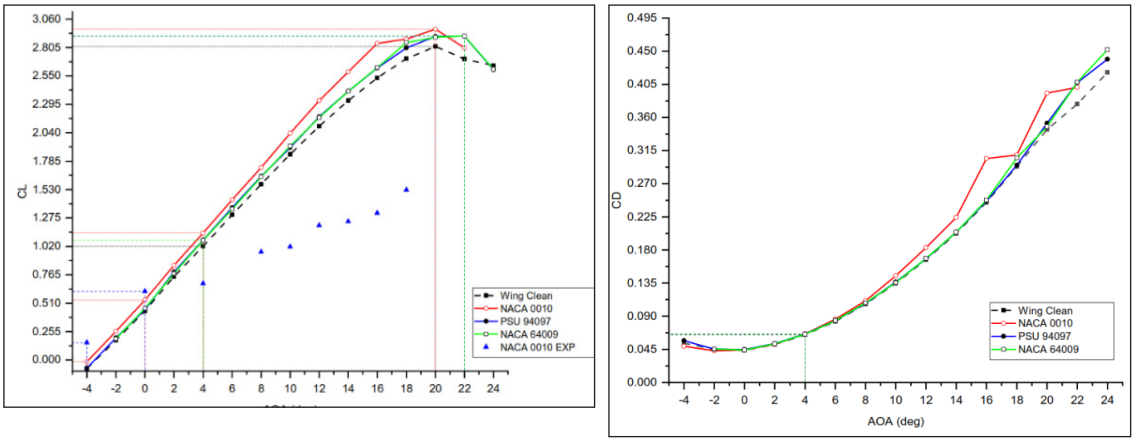

(a) Wing Lift Coefficient Comparison (with validation)

(b) Wing Drag Coefficient Comparison

Figure 3-2. Comparison of Coefficient Lift and Drag of Various Airfoil Sections

Figure 3-2 (b) shows a comparison of drag coefficients. The winglet with PSU 94097 airfoil has lower drag but higher lift than the clean wing configuration. In general, this proves that the addition of winglets can reduce induced drag and increase lift. However, it also shows that the winglet chord line length has an optimal value as well although it only has a slight impact on decreasing drag and increasing lift. With an increase in the angle of attack, drag and lift will also increase, but the increase of the wing with the addition of winglets does not show a linear increase as the clean wing configurations.

Figure 3-3 shows a comparison of wing lift to drag ratio between a clean wing and 3 winglet configurations. Consistent with the lift and drag curve, the NACA 0010 airfoil gives a higher lift-to ratio than others. The cambered airfoil gives a balanced value between its L/D ratio.

Figure 3-4 shows a comparison of clean wing and winglet configuration on drag polar parameters. A drag polar curve is used on prediction of aircraft performance.

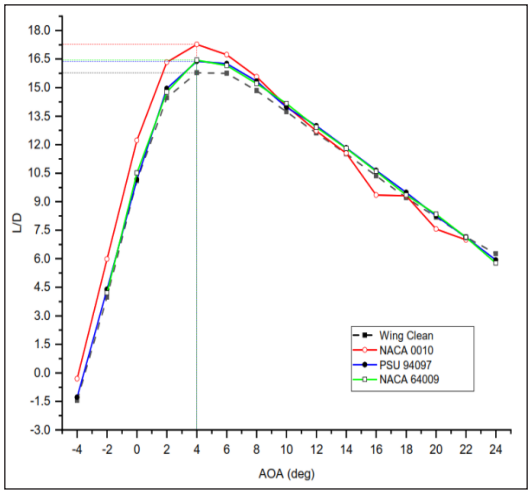

Figure 3-3. Comparison of wing L/D ratio

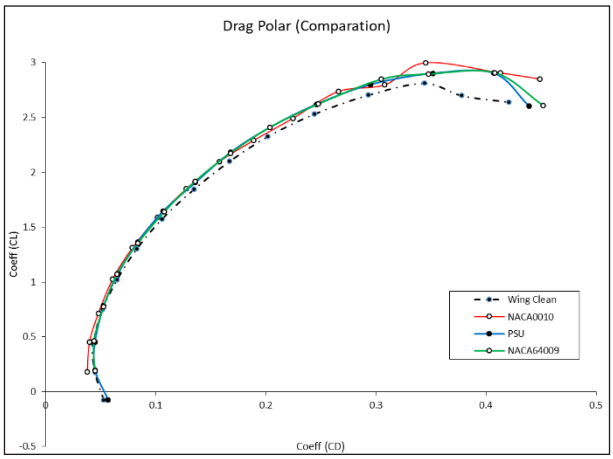

Figure 3-4. Comparison of wing drag polar

Induced drag is the drag resulting from the limitation of the wing (infinite wing) in generating lift. For lift to be generated, a pressure difference between the lower surface of the wing and the upper surface of the wing must exist. When this pressure difference tends to balance each other, airflow occurs at the wing tip.

From Fig. 3-4, the graph of polar drag against an angle of attack on the aircraft wing of the aircraft after the addition of winglets, there is an overall increase in the drag coefficient value. However, it can also be observed that the value of induced drag has decreased. In accordance with the purpose of adding winglets, namely reducing induced drag, where the total drag is the total result of profile drag and induced drag. In addition, with the addition of winglets, there is an increase in the elevator coefficient on the aircraft. The drag polar curve is presented to show the contribution of induced drag that has been reduced due to winglet installation.

3.3. Aerodynamics Characteristic Comparison and Analysis

Certain parameters of aerodynamic characteristics from simulation results are compared to determine the optimum configuration of winglet design with airfoil cross-section. The parameters are wing lift-to-drag ratio. Table 3-2. shows a comparison of all configurations on aerodynamic parameters.

Table 3-2. Comparison of Coefficient Lift and Drag of Various Airfoil Sections

Winglet Config	AOA (deg)	Angle of Stall (deg)	Cl_{max}	L/D	% (L/D)
Wing Clean	4	20	2.814	15.77	0.0
NACA 0010	4	20	2.970	17.27	9.5
NACA 64009	4	22	2.908	16.44	4.2
PSU 94097	4	22	2.906	16.38	3.8

The simulation results show that when the winglet is installed on the wing, both lift-to-drag ratio parameters are increasing, calculated as a percentage of the clean wing configuration. By comparing all winglet configurations. The NACA 0010 has an optimum value in the lift-to-drag ratio, gaining a 9.5% improvement compared to a clean wing configuration. The symmetric profile of the NACA 0010 generates more additional lift than the cambered airfoil profiles of NACA 64009 and PSU 94097 which gain around a 4% improvement. The stall angle differences should also be noted. The cambered airfoil configuration tends to have a higher value than a clean wing and NACA 0010 configuration. It is at 22 degrees of stall angle.

4. Conclusions

The comparison between airfoil profiles shows a marginal difference in both lift-to-drag ratio. The lift-to-drag ratio and the higher stall angle represent the aerodynamic efficiency of wing design. Overall, the addition of winglets increases lift, reduces the induced drag, and delays the stall phenomena of the wing. On analyzing the relation between aerodynamic performance and the airfoil shape or profile. Although the NACA 0010 has a symmetrical shape, the thickness of its airfoil tends to increase aerodynamic efficiency than a cambered shape airfoil. One of the winglet design is to gain improvement by producing more lift and reduce induced drag. Therefore, thickness gives a significant influence by increasing the lift-to-drag ratio. The future study and simulations should be conducted to optimize the shape of the winglet airfoil profile that gains a benefit from thickness and a cambered shape.

Acknowledgements

The author would like to thank the head of Technology Research Center for Aeronautics – BRIN, for the facilities support for this research activity.

Contributorship Statement

All authors are the main contributors. STP and ARS prepared the manuscript; MF and TMIH analyzed the test results; KH conducted the experimental test, JAH prepared test plans and experimental test, and MLR developed the drawings.

References

Sadraey, M.H., *Aircraft Design: A Systems Engineering Approach*. 2012, John Wiley & Sons, Ltd: New Hampshire, USA.

Tirtha, S., et al., *Studi Eksperimental Perangkat Ujung Sayap Pada Pesawat 19 Penumpang.* Jurnal Teknologi Penerbangan (Approach), 2020. 4(1).

Rabbi, M., R. Nandi, and M. Mashud, *Induce drag reduction of an airplane wing.* American Journal of Engineering Research, 2015. 4: p. 219-223.

Altab, H., et al., *Drag analysis of an aircraft wing model with and without bird feather like winglet.* International Journal of Aerospace and Mechanical Engineering, 2012. 6: p. 8-13.

Sidairi, K.A. and G.R. Rameshkumar, *Design of Winglet for Aircraft.* International Journal of Multidisciplinary Sciences and Engineering, 2016. 7(1).

Sawale, A., M.D. Khaleel, and S. Jaswanth, *Design and Analysis of Winglet.* International Journal of Civil Engineering and Technology (IJCIET), 2017. 8(5): p. 842-850.

Guha, T.K., W. Oates, and R. Kumar, *Characterization of Piezoelectric Macrofiber Composite Actuated Winglets.* Smart Materials and Structures, 2015. 24.

Whitcomb, R.T., *A Design Approach and Selected Wind Tunnel Results at High Subsonic Speed for Wing-Tip Mounted Winglets*. 1976, NASA: Virginia, USA.

Verrastro, M. and I. Dimino, *Chapter 21 - Morphing Devices: Safety, Reliability, and Certification Prospects*, in *Morphing Wing Technologies*, A. Concilio, et al., Editors. 2018, Butterworth-Heinemann. p. 647-682.

Ravi, S., A. N, and N.P. Kishore, *Performance Analysis of Winglet at Different Angle of Atack.* International Research Journal of Engineering and Technology (IRJET), 2016. 3(9).

Kim, Y. and S. Kim, *Analysis for aerodynamics of the simplified model of a commercial airplane cruising at transonic speed.* Journal of Engineering Science and Technology, 2010. 5.

Krog, L., et al., *Topology Optimisation of Aircraft Wing Box Ribs*, in *10th AIAA/ISSMO Multidisciplinary Analysis and Optimization Conference, 2004*.

Bontoft, E.K. and V. Toropov, *Topology Optimisation of Multi-Element Wingtip Devices*, in *2018 AIAA/ASCE/AHS/ASC Structures, Structural Dynamics, and Materials Conference*.

Singh, G., V. Toropov, and J. Eves, *Topology Optimization of a Blended-Wing-Body Aircraft Structure*, in *17th AIAA/ISSMO Multidisciplinary Analysis and Optimization Conference, 2016*.

Teixeira, M., F. Goulart, and F. Campelo, *Evolutionary Multiobjective Optimization of Winglets*. 2016. 1021-1028.

Maughmer, M., T. Swan, and S. Willits, *Design and Testing of a Winglet Airfoil for Low-Speed Aircraft.* Journal of Aircraft - J AIRCRAFT, 2002. 39: p. 654-661.

Mathew, B.C., A. Thakan, and J.V. Muruga Lal Jeyan, *A review on Aerodynamic performance of NACA Airfoil for various Reynolds number.* Journal of Physics: Conference Series, 2020. 1473(1): p. 012003.

Lehmkuehler, K., *Winglet Design for a Fairchild Merlin III using CFD Analysis*. 2015.

Anderson, J.D., *Fundamentals of Aerodynamics*. 6th ed. 2017, New York: McGraw-Hill.

Hamonangan, J.A. and A. Fajrin, *Penentuan Faktor Koreksi Kalibrasi : Kalibrasi Eksternal Balance Terowongan Angin Subsonik LAPAN*, in *Teknologi Pesawat Terbang : sebagai mitra pengembang Teknologi Roket dan Satelit Nasional*, A. Bintoro, et al., Editors. 2015, Indonesia Book Project: Jakarta. p. 3-14.

Aribowo, Agus, et al. *"Perancangan Wingtip Device Pesawat N-219 Untuk Meningkatkan Efisiensi Sayap."* Prosiding SIPTEKGAN XVI-2012 Seminar Nasional IPTEK Dirgantara XVI Tahun 2012. Pusat Teknologi Penerbangan, 2012.